

## Laccase-catalyzed synthesis of polypyrrole-multiwalled carbon nanotube composites as energy storage materials for capacitors

Junghee Park, Nasrin Raseda, Eun Suok Oh, Keungarp Ryu

Department of Chemical Engineering, College of Engineering, University of Ulsan, Ulsan 44610, Korea

Correspondence to: K. Ryu (E-mail: kgryu@mail.ulsan.ac.kr)

**ABSTRACT:** Multiwalled carbon nanotubes (MWNTs) were coated with polypyrrole (PPy) using *in situ* enzymatic polymerization of pyrrole catalyzed by a laccase (benzenediol:oxygen oxidoreductase, EC 1.10.3.2) from *Trametes versicolor*. Transmission electron microscopy revealed that the MWNTs were uniformly coated with very thin layers of PPy without any indication of globular polymer aggregate formations. The enzymatic synthesis of the MWNTs/PPy composites was quite simple being performed in a one-pot aqueous solution (pH 4.0) under mild reaction conditions. The potential of the composites with respect to the development of energy storage devices was demonstrated by fabricating a two-electrode coin cell capacitor (diameter 20 mm, thickness 1.6 mm) utilizing the composites as electrode materials. The capacitance of the cell was  $28.0 \text{ F g}^{-1}$  for the electrode material as measured by a galvanostatic charge–discharge method. The energy density and power density were 2.55 and  $805 \text{ W kg}^{-1}$ , respectively, which were close to those of the capacitors classified as ultracapacitors. © 2015 Wiley Periodicals, Inc. *J. Appl. Polym. Sci.* **2016**, *133*, 43307.

**KEYWORDS:** coatings; conducting polymers; electrochemistry; nonpolymeric materials and composites

Received 16 October 2015; accepted 3 December 2015

DOI: 10.1002/app.43307

### INTRODUCTION

The composite materials consisting of carbon nanotubes (CNTs) and conducting polymers possess combined advantages of both CNTs and conducting polymers.<sup>1</sup> CNTs including multiwalled carbon nanotubes (MWNTs) and single walled carbon nanotubes are known to have excellent chemical resistance, good mechanical strength, high electrical conductivity, and large surface areas.<sup>2,3</sup> On the other hand, conducting polymers such as polyanilines, polypyrroles (PPy), and polythiophenes have high pseudocapacitances.<sup>1</sup> Thus, CNTs/conducting polymer composites have been acknowledged to have great potential as energy storage materials in supercapacitors, various amperometric biosensors,<sup>4,5</sup> and electrolytic production of hydrogen.<sup>6</sup>

To date, CNTs/conducting polymer composites have been synthesized by either *in situ* chemical or electrochemical polymerization of monomers in the presence of carbon nanotubes acting as scaffolds.<sup>7–11</sup> In the chemical synthetic methods of the composites, strong oxidants, such as ammonium peroxydisulfate are often used as catalysts which can lead to the damaging of intact structures of CNTs and co-production of conducting polymer aggregates due to the presence of unavoidable solution-phase polymerization.<sup>7,8</sup> These drawbacks of chemical synthetic methods can deteriorate the performance of the composites.

Unlike chemical synthetic methods, enzymatic polymerization methods can be carried out under mild conditions, therefore, are environmentally friendly in that they do not require toxic oxidants or result in the formation of hazardous byproducts. A variety of polymers including polyesters, polylactones, polyphenols, and conducting polymers have been synthesized by peroxidases, laccases, and lipases, among others.<sup>12–16</sup> For example, carboxylated CNTs have been employed as templates to enhance the synthesis of conducting polyanilines.<sup>17</sup> Until now, however, enzymatic catalysis has scarcely been investigated to synthesize CNTs/conducting polymer composites.

CNTs/conducting polymer composites for which CNTs are uniformly coated with conducting polymers are crucial for the development of high performance energy storage materials since their highly porous entangled networks are expected to facilitate the efficient transfer of ions and electrolytes.<sup>18</sup> Preparation of such composites has been previously reported by using the concomitant *in situ* electrochemical synthesis and deposition of PPy on the surface of MWNTs at the electrodes<sup>10,19,20</sup> as well as chemical polymerization of monomers previously adsorbed on the surfaces of carboxylated MWNTs.<sup>18</sup> Most enzymes tend to physically adsorb onto CNTs at high loadings.<sup>21</sup> Thus, utilizing enzymes that spontaneously adsorb onto CNTs to synthesize CNTs/conducting polymer composites may enable the uniform coating of CNTs with conducting polymers since enzymatic

polymerization reactions are expected to be restricted on the surface of CNTs with negligible occurrence of solution-phase polymerization. Compared to chemical or electrochemical synthetic methods, the enzymatic synthesis of CNTs/conducting polymer composites is simple and can be performed in a one-pot system without the requirement for prior surface modification of CNTs and the adsorption of monomers on the modified CNTs.

We previously reported that horseradish peroxidase can catalyze the synthesis of MWNTs/PPy composites with  $H_2O_2$  as an oxidizing agent. Specifically, in the synthesized MWNTs/PPy composites, the MWNTs are uniformly coated with PPy in the absence of PPy aggregates.<sup>22</sup> Laccases (EC 1.10.3.2) are multicopper containing oxygen oxidoreductases that can catalyze the oxidation of various organic and inorganic compounds with molecular oxygen instead of  $H_2O_2$ .<sup>23,24</sup> Laccases have also been employed to synthesize various polymers including conducting polymers.<sup>25,26</sup> The mechanism of laccase-catalyzed polymerization of pyrrole is known to be similar to the electrochemical and chemical polymerization mechanisms:<sup>26</sup> for the reduction of each oxygen molecule to water, four pyrrole molecules are oxidized to the corresponding cationic radicals. Then, the cationic radicals undergo subsequent coupling steps to form dimers releasing two protons for each dimer. Dimers and oligomers of pyrroles are also known to be oxidized by laccase leading to the growth of the pyrrole polymers.

In this paper, we report a laccase-catalyzed synthesis of MWNTs/PPy composites for which PPy forms very thin uniform coatings on MWNTs. The resulting composites were tested for their suitability as electrode materials in symmetric two-electrode coin cell capacitors.

## EXPERIMENTAL

### Materials

MWNTs of 95% purity prepared by the chemical vapor deposition method were obtained from Hanwha Nanotech (Korea). The MWNTs were 10–15 nm in diameter and 10–20  $\mu\text{m}$  in length. Laccase (Sigma 53739) purified from *Trametes versicolor* and other chemicals were purchased from Sigma-Aldrich and used without further purification. The laccase used in this study was previously found to be pure by both native-PAGE<sup>27</sup> and sodium dodecyl sulfate (SDS)-PAGE<sup>28</sup> analyses and has an estimated molecular weight of 66 kDa.

### Enzymatic Synthesis and Characterization of MWNTs/PPy Composites

The laccase-catalyzed *in situ* synthesis of MWNTs/PPy composites was performed as follows. To a 20 mL citrate-phosphate buffer (pH 4, 100 mM), 100 mg MWNTs and 2 mg laccase were added and shaken for 30 min to adsorb laccase onto the MWNTs. Next, 135 mg (100 mM) pyrrole and 1.1 mg (0.1 mM) 2,2'-azinobis (3-ethylbenzothiazoline-6-sulfonate) (ABTS) as a redox mediator were added to the mixture to initiate the synthesis of PPy. ABTS was previously shown to increase the synthetic yield of PPy with horseradish peroxidase as a catalyst.<sup>22</sup> The reaction mixture was gently shaken at 4°C for 24 h. The aqueous buffer was saturated with air by bubbling air

stream before the reaction. After the reaction was finished, the reaction mixture was filtered with a nylon membrane (0.2  $\mu\text{m}$ , Whatman) and then the composites were washed with copious amounts of distilled water and 50 v/v % methanol. The final MWNTs/PPy composites were dried under vacuum at 60°C and stored for further uses. The yield of PPy was calculated gravimetrically from the difference between the mass of the MWNTs initially added to the reaction mixture and the total mass of the final dry composites. The synthetic yield of PPy was 25.5% of the initial amounts of pyrrole monomer.

To identify and verify the synthesis of PPy, Fourier transform infrared (FTIR) spectroscopy was performed with a Nicolet 380 FTIR spectrometer (Thermo Electron). The wave number range of FTIR was from 500 to 4000  $\text{cm}^{-1}$  at a 2  $\text{cm}^{-1}$  resolution. Samples were mixed with potassium bromide using a mortar and a pestle, then compressed into pellets. Pellets of pure potassium bromide were used as blank samples.

### Fabrication of Two-Electrode Coin Cell Capacitors and Electrochemical Measurements

The potential of MWNTs/PPy composites as energy storage materials was evaluated by fabricating two-electrode coin cells as capacitors (CR2016 stainless steel coin cell, diameter 20 mm, thickness 1.6 mm) and measuring their electrical capacitances. To prepare electrode materials, 16 mg MWNTs/PPy composites (or pristine MWNTs as a control), 2 mg carbon black, and 20 mg *n*-methyl-2-pyrrolidinone (NMP) solution containing 10 wt % polyvinylidene difluoride (PVDF) were mixed together by a ball mill. The ball milled mixture was then coated evenly on the inner surface of the coin cells. Typically, approximately 5.0 mg of the electrode material was coated on each electrode. The coated coin cells were dried at 120°C for 1.5 h. Next, the coated dried coin cells were pressed together with a crimper to fabricate the capacitors. A glass membrane filter was used to separate the two electrodes and a 1M  $\text{NaNO}_3$  aqueous solution was used as an electrolyte.<sup>10</sup> The coin cell capacitors were stabilized at room temperature for 1 h before measuring the electrochemical properties. Cyclic voltammetry and the galvanostatic charge-discharge method (discharge current = 1 mA) were carried out to measure the capacitances of the coin cell capacitors using a potentiostat/galvanostat (PHE200, Garmry Instruments).

## RESULTS AND DISCUSSION

### Laccase-Catalyzed Synthesis and Structural Investigation of MWNTs/PPy Composites

Figure 1 shows a schematic of the laccase-catalyzed one-pot *in situ* polymerization of pyrrole (100 mM) in the presence of MWNTs used to prepare MWNTs/PPy composites. First, laccase (2 mg) was added to a buffer solution containing MWNTs (100 mg) followed by the gentle shaking of the mixture to allow spontaneous adsorption of enzyme molecules onto the surfaces of the MWNTs. The amounts of laccase mixed with MWNTs was far below the adsorption level of the enzymes on MWNTs<sup>29</sup> to ensure the maximum adsorption of the enzyme. Pyrrole monomers were, subsequently, added to the mixture to initiate the polymerization reaction.

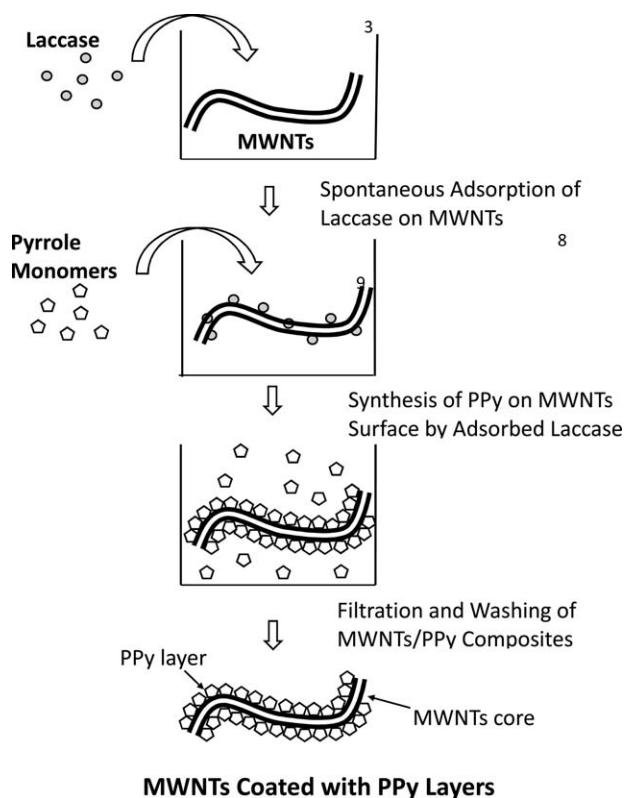


**Figure 1.** Schematic process for the laccase-catalyzed one-pot synthesis of MWNTs/PPy composites.

Importantly, the adsorbed laccase on the MWNTs was expected to catalyze the synthesis of PPy resulting in its growth in layers on the surface of the MWNTs.

Scanning electron microscopy (SEM) was performed on a microscope (Supra 40, Carl Zeiss, Swiss) to examine the morphology of the MWNTs/PPy composites synthesized by laccase. SEM image of pristine MWNTs showed that the MWNTs fibers were slightly transparent with clean smooth surfaces [Figure 2(a)]. On the other hand, the SEM image of MWNTs/PPy composites synthesized by laccase showed that the MWNTs/PPy composites became less transparent and surfaces were not as smooth as those of pristine MWNTs [Figure 2(b)]. The differences between the SEM images in Figure 2 implied that the MWNTs were uniformly coated by PPy layers. As was also previously reported for the synthesis of MWNTs/PPy composites by horseradish peroxidase,<sup>22</sup> globular aggregates of PPy that were formed in the absence of MWNTs were not observed for the MWNTs/PPy composites synthesized by the laccase. This result indicates that PPy was synthesized only on the surface of MWNTs by adsorbed laccase on MWNTs. We also noted that the MWNTs strongly adsorbed more than 10 wt % of the laccase, implying that most of the laccase (2 mg) used in this reaction mixture was bound to the MWNTs (100 mg).<sup>29</sup> Therefore, the growth of the globular PPy aggregates by the laccase dissolved in the bulk solution became negligible. On the contrary, chemical synthesis of MWNTs/PPy composites was reported to result in large quantities of globular aggregates of PPy in composites due to the inability to prevent solution-phase polymer-

ization of PPy.<sup>7</sup> To minimize the formation of polymer aggregates in chemical synthetic methods, MWNTs should be modified to introduce surface carboxylic acid groups in order to facilitate subsequent adsorption of monomers on the modified MWNTs.<sup>18</sup> Furthermore, compared to these multistep chemical procedures, enzymatic processes are simple. The presence of the globular PPy aggregates in the composites may decrease the surface area of the MWNTs network structure, and subsequently deteriorates the performance of composites as energy storage materials. It is also worth noting that during the mild enzymatic synthesis of MWNTs/PPy composites, the intact fibrous network structure of MWNTs remained unharmed without being fragmented or damaged, in contrast to the chemical synthesis of the composites. Such retention of intact structures of MWNTs in the final composites is necessary to achieve better electrochemical performance of the composites.

Transmission electron microscopy (TEM) was performed on a microscope (JEM 2100, JEOL, Japan) for further verification of the uniform coverage of the MWNTs by PPy layers. Figures 3 and 4 compare the TEM images of pristine MWNTs without PPy to that of the MWNTs/PPy composites synthesized by laccase. As shown in Figure 3, the surface of pristine MWNTs was smooth and clean, whereas Figure 4 shows that the MWNTs/PPy composites were evenly coated with very thin layers of PPy.

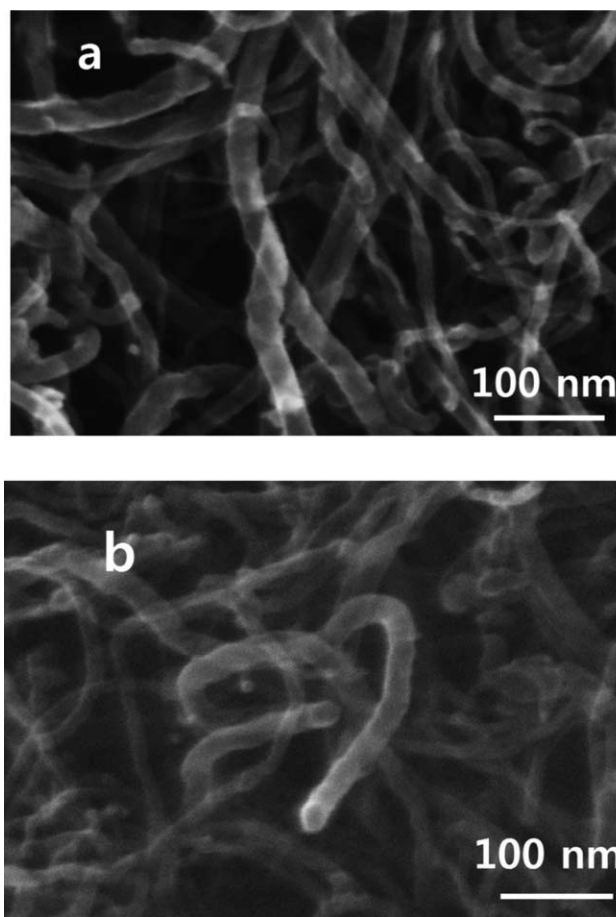


**Figure 2.** SEM images of pristine MWNTs (a) and MWNTs/PPy composites synthesized by laccase (b).

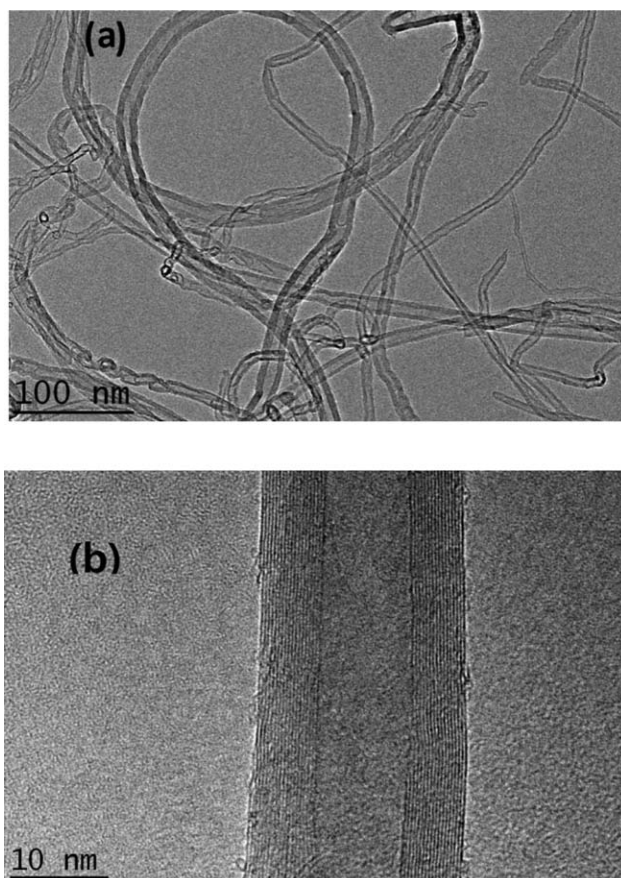


**Figure 3.** TEM images of pristine MWNTs with low (a) and high (b) magnifications.

The thickness of the PPy layers was visually estimated to be less than 3–4 nm. The TEM image of the composites in Figure 4(a) shows widespread tiny spots. According to our previous study, the morphology of PPy synthesized by horseradish peroxidase without MWNTs was the aggregates of globules the size of which was about 100 nm in diameter, therefore, much larger than the spots.<sup>22</sup> Additionally, such spots were not visible in the TEM images of the MWNTs/PPy composites taken after the harsh ball-milling process (images not shown). Based on these aspects, we presume that these background spots are not directly related to either the composites or PPy aggregates.

Fourier transform infrared spectroscopy (FTIR) was carried out to investigate the chemical nature of the MWNTs/PPy composites. Figure 5 shows the FTIR spectrum of MWNTs/PPy composites, which exhibited many characteristic absorption peaks of the FTIR pattern of PPy (3400  $\text{cm}^{-1}$ , stretching vibration of N–H bonds; 1560  $\text{cm}^{-1}$ , stretching vibration of C=C bonds; 1045 and 1304  $\text{cm}^{-1}$ , inplane vibrations of C–H bonds; 940  $\text{cm}^{-1}$ , C–C bond vibration; 790  $\text{cm}^{-1}$ , out-of-plane vibrations of the C–H bonds).<sup>30–32</sup> The peak at 2400  $\text{cm}^{-1}$  is due to  $\text{CO}_2$ , which happened to be entrained with air into the FTIR pellets.<sup>33</sup> On the contrary, the FTIR spectrum of the pristine MWNTs lacked these characteristic absorption peaks near 3400  $\text{cm}^{-1}$  and between 1500 and 500  $\text{cm}^{-1}$ .

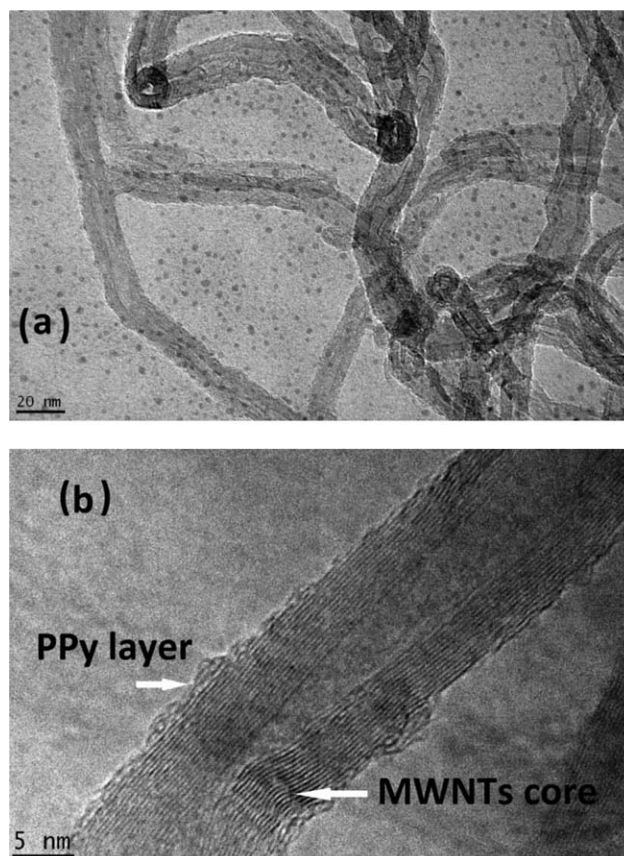


**Figure 4.** TEM images of MWNTs/PPy composites synthesized by laccase with low (a) and high (b) magnifications.

#### Electrochemical Capacitances of the MWNTs/PPy Composites

Two-electrode capacitors have been reported to be useful in characterizing the electrochemical properties of electrode materials.<sup>7</sup> Accordingly, we fabricated a coin-cell capacitor using a crimper, which has two symmetric electrodes as shown in Figure 6. Typically, electrodes of composites have been prepared by coating the composite-binder mixtures on thin metal foils under high pressures and temperatures<sup>9,18</sup> or forming pellets of the mixtures by pressing under extremely high pressures.<sup>34,35</sup> In

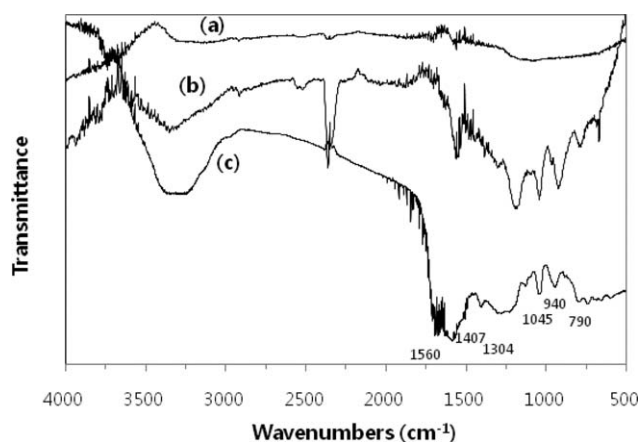


**Figure 5.** FTIR spectra of pristine MWNTs (a), MWNTs/PPy composites (b), and PPy (c).

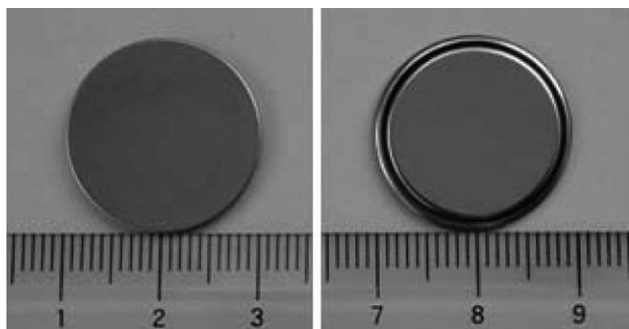


**Figure 6.** Photographs of fabricated two-electrode coin cells after crimping.

this study, we simply deposited and spread electrode materials on the inner surfaces of the coins, then dried the electrodes. This simple method of electrode preparation was performed under mild ambient conditions. Thereby, the inner surfaces of the two coins were evenly coated with either MWNTs/PPy composites (80 wt % MWNTs/PPy composites, 10 wt % carbon black, 10 wt % PVDF) or pristine MWNTs (80 wt % MWNTs, 10 wt % carbon black, 10 wt % PVDF) as a blank. The effects of ball milling process on the structure of the MWNTs/PPy composites were investigated by TEM (images not shown). The TEM images of the composites taken after ball milling clearly showed that the structure of the composites remained intact without fragmentation of MWNTs or the detachment of PPy layers from MWNTs.

Subsequently, the electrical energy storage capacitance of the coin cell was measured by cyclic voltammetry and the galvanostatic charge–discharge method. Specific capacitance  $C_{sp}$  ( $F g^{-1}$ ) was defined as the capacitance of the cell per unit mass of materials coated on one electrode and calculated from cyclic voltammetry data using the following equation<sup>36</sup>:

$$C_{sp} = \frac{S}{2\Delta V}$$

where  $S$  is the area of a closed cyclic voltammetry curve for instantaneous capacitance  $C_i$  ( $F g^{-1}$ ) versus voltage and  $\Delta V$  is the difference between the maximum and minimum voltages. The  $C_i$  value was calculated from the initial CV curve for the current (ampere) versus voltage by the equation:

$$C_i = \frac{2i}{m \times s}$$

where  $i$  is the current,  $m$  is the total mass of the electrode materials coated on both electrodes, and  $s$  is the voltage scan rate.

Figure 7 shows the CV curves ( $C_i$  versus voltage) for MWNTs/PPy composites at different scan rates (20, 50, and 100  $mV s^{-1}$ ) as well as for PPy alone and pristine MWNTs at 50  $mV s^{-1}$  as controls. The shapes of the CV curves for an ideal capacitor are known to be rectangular and independent of the voltage scan rates. On the other hand, the CV curves for the coin cell capacitors developed in this study had rounded ends and varied slightly according to different scan rates due to the nonideal behavior of the cell. No obvious redox peaks were observed in CV curves indicating the

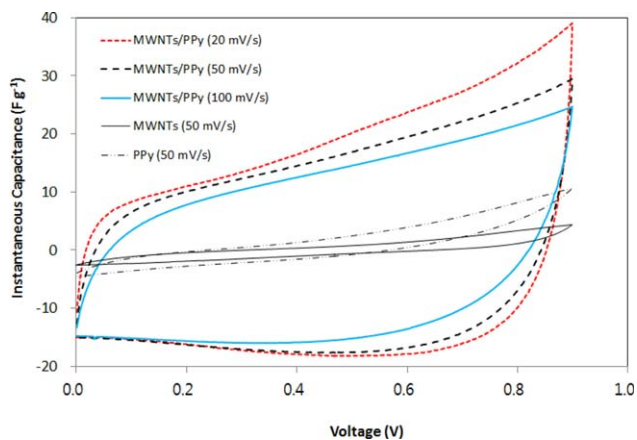


**Figure 7.** Cyclic voltammograms of PPy alone, pristine MWNTs, and MWNTs/PPy composites. Cyclic voltammetry was performed at potentials between 0.0 and 0.9 V. [Color figure can be viewed in the online issue, which is available at wileyonlinelibrary.com.]

absence of strong redox reactions in the capacitors. The  $C_{sp}$  values for MWNTs/PPy composites calculated from the CV curves were 13.1–17.4  $F g^{-1}$  (Table I). In addition, Figure 7 and Table I show that PPy alone and MWNTs without PPy layers had negligible capacitances. Therefore, to obtain high capacitance, nanoporous structures of MWNTs combined with high capacitance of PPy are essential to facilitate electron and ion transfer processes.

The specific capacitances of the capacitors were also measured by the galvanostatic charge–discharge experiment<sup>36</sup>:

$$C_{sp} = \frac{4i \times t_d}{\Delta V \times m}$$

where  $i$  is the current loaded (ampere),  $t_d$  is the discharge period (s), and  $\Delta V$  is the voltage change during the discharge step. As shown in Figure 8, the galvanostatic discharge curve for the coin cell capacitor was linear, indicating the capacitive property of the coin cell.<sup>19</sup> The  $C_{sp}$  value for MWNTs/PPy composites was calculated to be 28.0  $F g^{-1}$ .

Finally, the energy density  $E$  ( $Wh kg^{-1}$ ) and the power density  $P$  ( $W kg^{-1}$ ) were calculated from the following equations,

**Table I.** Capacitances of Two Electrode Coin Cell Capacitors Measured by Cyclic Voltammetry

Electrode materials <sup>a</sup>	Scan rate ( $mV s^{-1}$ )	Capacitance ( $F g^{-1}$ ) <sup>c</sup>
Pristine MWNTs	50	0.9
PPy globules <sup>b</sup>	50	1.6
MWNTs/PPy composites	20	17.4
MWNTs/PPy composites	50	15.1
MWNTs/PPy composites	100	13.1

<sup>a</sup> Approximately, 5 mg material was deposited on each electrode.

<sup>b</sup> PPy globules were synthesized by laccase in the absence of MWNTs under the same reaction conditions as described in the text.

<sup>c</sup> Data are the averages of triplicate measurements with errors less than 5.0%.

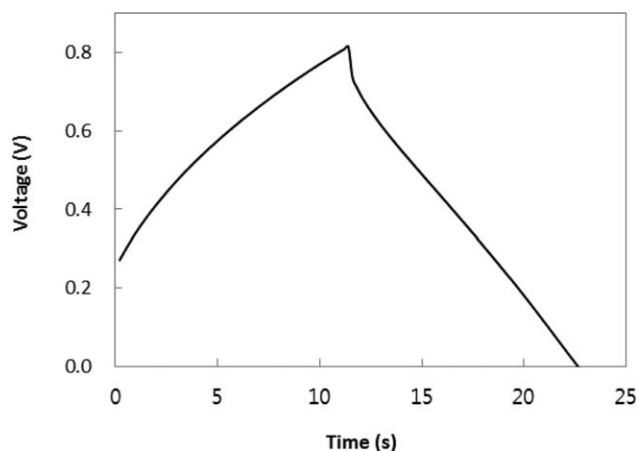


**Figure 8.** Galvanostatic charge–discharge curve of MWNTs/PPy composites. The discharge current was 1 mA.

respectively, to assess the operational capability of the coin cell as a capacitor<sup>11,37</sup>:

$$E = \frac{C_{sp} \times V_m^2}{2}$$

$$P = \frac{E}{t_d}$$

where  $V_m$  is the maximum voltage in the galvanostatic charge–discharge plot. The values of  $E$  and  $P$  were determined to be 2.6 Wh kg<sup>-1</sup> and 805 W kg<sup>-1</sup>, respectively, based on the galvanostatic charge–discharge results. Importantly, these  $E$  and  $P$  values were close to those of the capacitors classified as ultracapacitors according to Ragone plots.<sup>38</sup>

## CONCLUSIONS

Laccase was successfully used to synthesize MWNTs/PPy composites for which the MWNTs were uniformly coated with very thin layers of PPy. The potential of the MWNTs/PPy composites as energy storage materials was demonstrated by fabricating a symmetric two-electrode coin cell capacitor. The measurement of electrochemical properties of the coin cell showed that the coin cell had the capacitance of approximately 28.0 F g<sup>-1</sup>. Based on the energy density and power density values, the coin cell performance was similar to that of the ultracapacitors.

## ACKNOWLEDGMENTS

This work was financially supported by a faculty research grant from the University of Ulsan, Korea (2014).

## REFERENCES

1. Frackowiak, E. *Phys. Chem. Chem. Phys.* **2007**, *9*, 1774.
2. Baibarac, M.; Gomez-Romero, P. *J. Nanosci. Nanotechnol.* **2006**, *6*, 289.
3. Lehman, J. H.; Terrones, M.; Mansfield, E.; Hurst, K. E.; Meunier, V. *Carbon* **2011**, *49*, 2581.
4. An, K. H.; Jeong, S. Y.; Hwang, H. R.; Lee, Y. H. *Adv. Mater.* **2004**, *16*, 1005.
5. Cheng, G.; Zhao, J.; Tu, Y.; He, P.; Fang, Y. *Anal. Chim. Acta* **2005**, *533*, 11.
6. Navarro-Flores, E.; Omanovic, S. *J. Mol. Catal. A Chem.* **2005**, *242*, 182.
7. Khomenko, V.; Frackowiak, E.; Beguin, F. *Electrochim. Acta* **2005**, *50*, 2499.
8. Konyushenko, E. N.; Stejskal, J.; Trchova, M.; Hradil, J.; Kovarova, J.; Prokes, J.; Cieslar, M.; Hwang, J. Y.; Chen, K. H.; Sapurina, I. *Polymer* **2006**, *47*, 5715.
9. Koysuren, O.; Du, C.; Pan, N.; Bayram, G. *J. Appl. Polym. Sci.* **2009**, *113*, 1070.
10. Hughes, M.; Shaffer, M. S. P.; Renouf, A. C.; Singh, C.; Chen, G. Z.; Fray, D.; Windle, J. A. H. *Adv. Mater.* **2002**, *14*, 382.
11. Wang, D. W.; Li, F.; Zhao, J.; Ren, W.; Chen, Z. G.; Tan, J.; Wu, Z. S.; Gentle, I.; Lu, G. Q.; Cheng, H. M. *ACS Nano* **2009**, *3*, 1745.
12. Gross, R. A.; Kumar, A.; Kalra, B. *Chem. Rev.* **2001**, *101*, 2097.
13. Alvarez, S.; Manolache, S.; Danes, F. *J. Appl. Polym. Sci.* **2003**, *88*, 369.
14. Nabid, M. R.; Entezami, A. A. *J. Appl. Polym. Sci.* **2004**, *94*, 254.
15. Ochoteco, E.; Mecerreyes, D. *Adv. Polym. Sci.* **2010**, *237*, 1.
16. Park, H.; Kwon, O. Y.; Ryu, K. *Kor. J. Chem. Eng.* **2015**, *32*, 1847.
17. Sheng, Q.; Zheng, J. *Biosens. Bioelectron.* **2009**, *24*, 1621.
18. Kong, L. B.; Zhang, J.; An, J. J.; Luo, Y. C.; Kang, L. J. *Mater. Sci.* **2008**, *43*, 3664.
19. Jurewicz, K.; Delpeux, S.; Bertagna, V.; Beguin, F.; Frackowiak, E. *Chem. Phys. Lett.* **2001**, *347*, 36.
20. Guo, D. J.; Li, H. L. *J. Solid State Electrochem.* **2005**, *9*, 445.
21. Davis, J. J.; Green, M. L. H.; Hill, H. A. O.; Leung, Y. C.; Sadler, P. J.; Sloan, J.; Xavier, A. V.; Tsang, S. C. *Inorg. Chim. Acta* **1998**, *272*, 261.
22. Ryu, K.; Xue, H.; Park, J. H. *J. Chem. Technol. Biotechnol.* **2013**, *88*, 788.
23. Piontek, K.; Antorini, M.; Choinowski, T. *J. Biol. Chem.* **2002**, *277*, 37663.
24. Madhavi, V.; Lele, S. S. *Bioresources* **2009**, *4*, 1694.
25. Karamyshev, A. V.; Shleev, S. V.; Koroleva, O. V.; Yaropolov, A. I.; Sakharov, I. Y. *Enzyme Microbial. Technol.* **2003**, *33*, 556.
26. Son, H. K.; Palmore, G. T. R. *J. Phys. Chem. B* **2005**, *109*, 19278.
27. Birhanli, E.; Yesilada, O. *Biochem. Eng. J.* **2010**, *52*, 33.
28. Raseda, N.; Hong, S.; Kwon, O. Y.; Ryu, K. *J. Microbiol. Biotechnol.* **2014**, *24*, 1673.
29. Park, J. H.; Xue, H.; Jung, J. S.; Ryu, K. *Kor. J. Chem. Eng.* **2012**, *29*, 1409.

30. Kupriyanovich, Y. N.; Sukhov, B. G.; Medvedeva, S. A.; Mikhaleva, A. I.; Vakulskaya, T. I.; Myachina, G. F.; Trofimov, B. A. *Mendeleev Commun.* **2008**, *18*, 56.
31. Qu, B.; Xu, Y. T.; Lin, S. J.; Zheng, Y. F.; Dai, L. Z. *Synth. Met.* **2010**, *160*, 732.
32. Sahoo, N. G.; Jung, Y. C.; So, H. H.; Cho, J. W. *Synth. Met.* **2007**, *157*, 374.
33. Yan, X. B.; Han, Z. J.; Yang, Y.; Tay, B. K. *J. Phys. Chem. C* **2007**, *111*, 4125.
34. Lota, K.; Khomenko, V.; Frackowiak, E. *J. Phys. Chem. Solids* **2004**, *65*, 295.
35. Deng, M.; Yang, B.; Hu, Y. *J. Mater. Sci.* **2005**, *40*, 5021.
36. Stroller, M. D.; Ruoff, R. S. *Energy Environ. Sci.* **2010**, *3*, 1294.
37. Choi, J. E.; Bae, G. Y.; Yang, J. M.; Lee, J. D. *Kor. Chem. Eng. Res.* **2013**, *51*, 308.
38. Li, X.; Wei, B. *Nano Energy* **2013**, *2*, 159.